Ocean Heat Transport as a Cause for Model Uncertainty in Projected Arctic Warming

IRINA MAHLSTEIN AND RETO KNUTTI

Institute for Atmospheric and Climate Science, ETH Zurich, Zurich, Switzerland

(Manuscript received 8 March 2010, in final form 27 September 2010)

ABSTRACT

The Arctic climate is governed by complex interactions and feedback mechanisms between the atmosphere, ocean, and solar radiation. One of its characteristic features, the Arctic sea ice, is very vulnerable to anthropogenically caused warming. Production and melting of sea ice is influenced by several physical processes. The authors show that the northward ocean heat transport is an important factor in the simulation of the sea ice extent in the current general circulation models. Those models that transport more energy to the Arctic show a stronger future warming, in the Arctic as well as globally. Larger heat transport to the Arctic, in particular in the Barents Sea, reduces the sea ice cover in this area. More radiation is then absorbed during summer months and is radiated back to the atmosphere in winter months. This process leads to an increase in the surface temperature and therefore to a stronger polar amplification. The models that show a larger global warming agree better with the observed sea ice extent in the Arctic. In general, these models also have a higher spatial resolution.

These results suggest that higher resolution and greater complexity are beneficial in simulating the processes relevant in the Arctic and that future warming in the high northern latitudes is likely to be near the upper range of model projections, consistent with recent evidence that many climate models underestimate Arctic sea ice decline.

1. Introduction

Anthropogenic greenhouse gases lead to a global warming of the climate system. The warming, however, is asymmetric: the high northern latitudes and landmasses show greater warming than the Southern Hemisphere and oceans due to ocean heat uptake (e.g., Flato and Boer 2001). It is the Arctic where the greatest warming is expected by the end of this century (e.g., Holland and Bitz 2003). Owing to differences in parameterizations and structural differences of the atmosphere–ocean global circulation models (AOGCMs), projections of future warming show large uncertainties.

The Arctic region is characterized by a very large variability and complex physical processes that govern its climate. Climate change caused by anthropogenic greenhouse gases impacts this region severely by changes in sea ice cover that have strong implications for the energy budget. Additionally, positive feedback mechanisms are key factors driving the Arctic warming (e.g., Manabe and Stouffer 1980). Numerous physical processes account for the strength of the ice albedo feedback, which is mainly responsible for the polar amplification (Deser et al. 2010). Polar warming is also strongly related to global warming, as depicted in Fig. 1, with a correlation of 0.87; that is, a higher global temperature increase implies a higher warming in the Arctic. Understanding the complex Arctic climate system with all its feedbacks is therefore indispensable to reduce some of the uncertainties in global climate change projections. This process is hampered by the fact that observations in the Arctic are sparse and thus large uncertainties exist in observational datasets. Hence, temperature projections in the Arctic comprise a larger spread [2.5–7.5 K for the Special Report on Emissions Scenarios (SRES) A1B for 2070–99 relative to 1970–99] of the AOGCMs than the global mean projections (1.8–4 K), at least in absolute terms.

As mentioned above, various physical processes influence future temperature projections but they are also important in simulating current climate and variability. Yet, it has proven difficult to find metrics based on

Corresponding author address: Irina Mahlstein, Institute for Atmospheric and Climate Science, ETH Zurich, Universitätstrasse 16, CH-8092 Zurich, Switzerland.
E-mail: irina.mahlstein@env.ethz.ch

DOI: 10.1175/2010JCLI3713.1

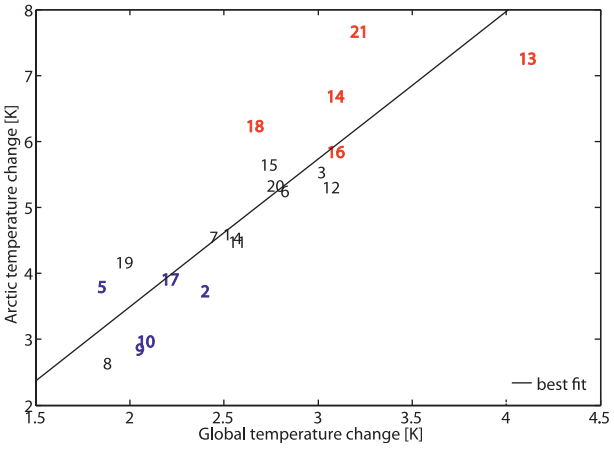

FIG. 1. Correlation ($R = 0.87$) across the CMIP3 models between the Arctic warming and the global warming (2070–99 relative to 1970–99). Numbers correspond to the models introduced in Table 1. Red (blue) labels mark the models that belong to the warm (cold) composite used in subsequent figures.

present-day mean climatology that strongly relate to future projections (Murphy et al. 2004; Tebaldi and Knutti 2007; Knutti et al. 2010; Knutti 2010), and the scientific community has struggled in many cases to define relevant metrics that would separate ''good'' from ''bad'' models, although there are some exceptions (Walsh et al. 2008; Wang and Overland 2009; Zhang 2010). Knutti et al. (2006) find a relation between the seasonal cycle in regional temperature and climate sensitivity. Hall (2004) shows that the strength of snow albedo feedback in spring is coupled to the strength of future temperature increase in each model. Physical processes such as the longwave feedback parameter of the models (Boé et al. 2009a) and the deep ocean heat uptake (Boé et al. 2009b) partly explain the large spread of future model projections in temperature. Simulating such processes properly and improving agreement with observations may be one possibility to reduce uncertainty in future projections. In this study we show that the main differences in the pattern of surface temperature in the Arctic are localized over the Barents Sea. This is a region where surface temperature depends on ocean currents, namely, the North Atlantic Drift Stream bringing warm surface water to high latitudes. The strength of the northward ocean heat transport impacts the sea ice cover in this region. Sea ice is a key player, causing a large albedo feedback, and together with the sea ice thickness feedback leads to a large Arctic warming. We show that process-based model evaluation can provide interesting insight into climate feedbacks and at the same time help to reduce model uncertainties.

2. Data and method

Different observational datasets are used for the evaluation of the models. The bias of the surface temperature (TAS) is compared to the 40-yr European Centre for Medium-Range Weather Forecasts Re-Analysis (ERA-40) dataset (Uppala et al. 2005). Though the newer product ERA-Interim exists, it is not used for the bias analysis because the dataset does not start before 1989 and, therefore, the time series is too short for a climatological analysis. Station data is very sparse in the Arctic and therefore ERA-40 is considered to be the most reliable to calculate the bias (Bromwich et al. 2007). The investigated period for TAS starts with 1970 and ends with 1999. For sea ice the Met Office Hadley Centre Sea Ice and Sea Surface Temperature (HadISST) dataset (Rayner et al. 2003) is used for comparison with model data. In this study only the period from 1980 to 2008 is considered.

The model dataset consists of up to 23 of the global coupled AOGCMs used for the Intergovernmental Panel on Climate Change (IPCC) Fourth Assessment Report (AR4) (Solomon et al. 2007), which are available from the World Climate Research Programme (WCRP) Coupled Model Intercomparison Project phase 3 (CMIP3) (Meehl et al. 2007). More information about the participating models is available on the Program for Climate Model Diagnosis and Intercomparison (PCMDI, available online at http://www-pcmdi.llnl.gov/about/index.php). All models providing the relevant data are included in the analysis except for the Flexible Global Ocean–Atmosphere–Land System Model gridpoint version 1.0 (FGOALS-g1.0). This model shows sea ice extent much larger than observed (Arzel et al. 2006). Since this study is focusing on the Arctic region, this model is excluded. The models used in this study are listed in Table 1. For all models and all variables, one ensemble member (run1) of the A1B scenario is used for the analysis. Not all modeling groups provide the ocean heat transport in the data archive. Therefore, for seven models the ocean heat transport is approximated by an energy balance as in Fig. 8.6 of Solomon et al. (2007).

All model data is regridded to a common T42 grid using a bilinear interpolation to be able to compare model results. Only for the northward ocean heat transport is the data used on the original grid to minimize issues with conservation of energy.

The projected warming is the difference between the mean TAS of the periods 2070–99 and 1970–99. For the evaluation of the models using observations, the period 1970–99 is used. For sea ice only the time period 1980–2008 is used when observations are included because the observational data is more reliable owing to use of

TABLE 1. CMIP3 models and data availability (**X**).

Number	Model	Sea ice	Ocean heat transport	Calculated ocean heat transport
1	BCCR-BCM2.0	**X**		**X**
2	CCCma CGCM3.1	**X**		**X**
3	CCCma CGCM3.1 T63	**X**		**X**
4	CNRM-CM3	**X**	**X**	
5	CSIRO Mk3.0	**X**	**X**	
6	GFDL CM2.0	**X**		**X**
7	GFDL CM2.1	**X**		
8	GISS-AOM	**X**	**X**	
9	GISS-EH			
10	GISS-ER	**X**	**X**	
11	INMCM3.0	**X**	**X**	
12	IPSL CM4	**X**		**X**
13	MIROC3.2 (hires)	**X**	**X**	
14	MIROC3.2(medres)	**X**	**X**	
15	MIUB-ECHO-G	**X**	**X**	
16	ECHAM5	**X**		**X**
17	MRI CGCM2.3.2a	**X**	**X**	
18	CCSM3.0	**X**	**X**	
19	PCM1			
20	UKMO HadCM3	**X**	**X**	
21	UKMO HadGEM1	**X**		**X**
22	CSIRO Mk3.5	**X**	**X**	

satellite techniques after 1980. The Arctic region in this study is defined as the area north of 60°N. Time averages are for the aforementioned periods, and spatial averages cover the region 60°–90°N throughout the paper.

3. Results and discussion

a. Surface temperature

To find a physical explanation for the large spread in global and the even larger spread in the Arctic warming, two different composites are constructed: one consisting of the five models with the largest warming in the Arctic (marked in red in Fig. 1) and the other consisting of the five models with the smallest Arctic warming (marked in blue in Fig. 1), excluding model 8 (see Table 2 for details of the two groups). This model is excluded from the composite because of the special behavior of its ocean heat transport and its warming (see section 3c).

Though selecting the members for the composites has a subjective component, sensitivity tests with more ''cold'' or ''warm'' models in the respective composites show that the results do not depend on the details of selecting the composites.

For these two composites, the mean surface temperature (TAS) over the period 1970–99 in April and September in the Arctic is calculated and the bias against the ERA-40 observational dataset is determined for each composite. Figure 2 shows that, in general, the warm composite reveals too warm temperatures compared to ERA-40, whereas the cold composite has a bias toward too low temperatures; that is, models with a warm (cold) current state show more (less) warming. It must be noted, however, that the ERA-40 shows a cold bias over the Arctic Ocean (Bromwich et al. 2007). This implies that the warm composite features a reduced warm bias; conversely, the bias of the cold composite may be even larger. The main differences are over the ocean and are most apparent over the Barents Sea, as is also stated by Chapman and Walsh (2007). Especially in September the differences between the two composites are particularly pronounced. The sea ice extent reaches its minimum at this time of the year and the ocean is capable of absorbing most energy at this time, while energy is radiated back to the atmosphere during winter, which enhances the large Arctic warming. Thus, differences in TAS in this region may strongly affect future warming in the polar region. Reasons for the large bias of both composites may be a complex feedback mechanism including sea ice cover and the associated ice albedo feedback, as well as the ocean heat transport. The details of this assumption will be discussed in the following sections.

TABLE 2. CMIP3 models of the two composites.

Warm models	Cold models
MIROC3.2(hires)	CCCma CGCM3.1
MIROC3.2 (medres)	GISS-EH
ECHAM5	GISS-ER
CCSM3.0	CSIRO Mk3.0
UKMO HadGEM1	MRI CGCM2.3.2a

b. Sea ice

Because large parts of the Arctic Ocean are covered with ice throughout the entire year, or part of it, and because the main differences are found over the ocean, the mean sea ice concentration is shown in Fig. 3 for the same two composites to investigate whether the differences arise from the sea ice cover. The Goddard Institute for Space Studies Model E-H (GISS-EH) is missing in the cold composite in the case of sea ice because data is not available. Note that, since the HadISST observational dataset is used, the period from 1980 to 2008 is examined. Figure 3 shows two interesting features. First, the composite using the warm models simulates the sea ice cover in April and September more accurately than the four cold models. Note that the conclusions are not dependent on the specific month in the year looked at. Second, the cold composite, not

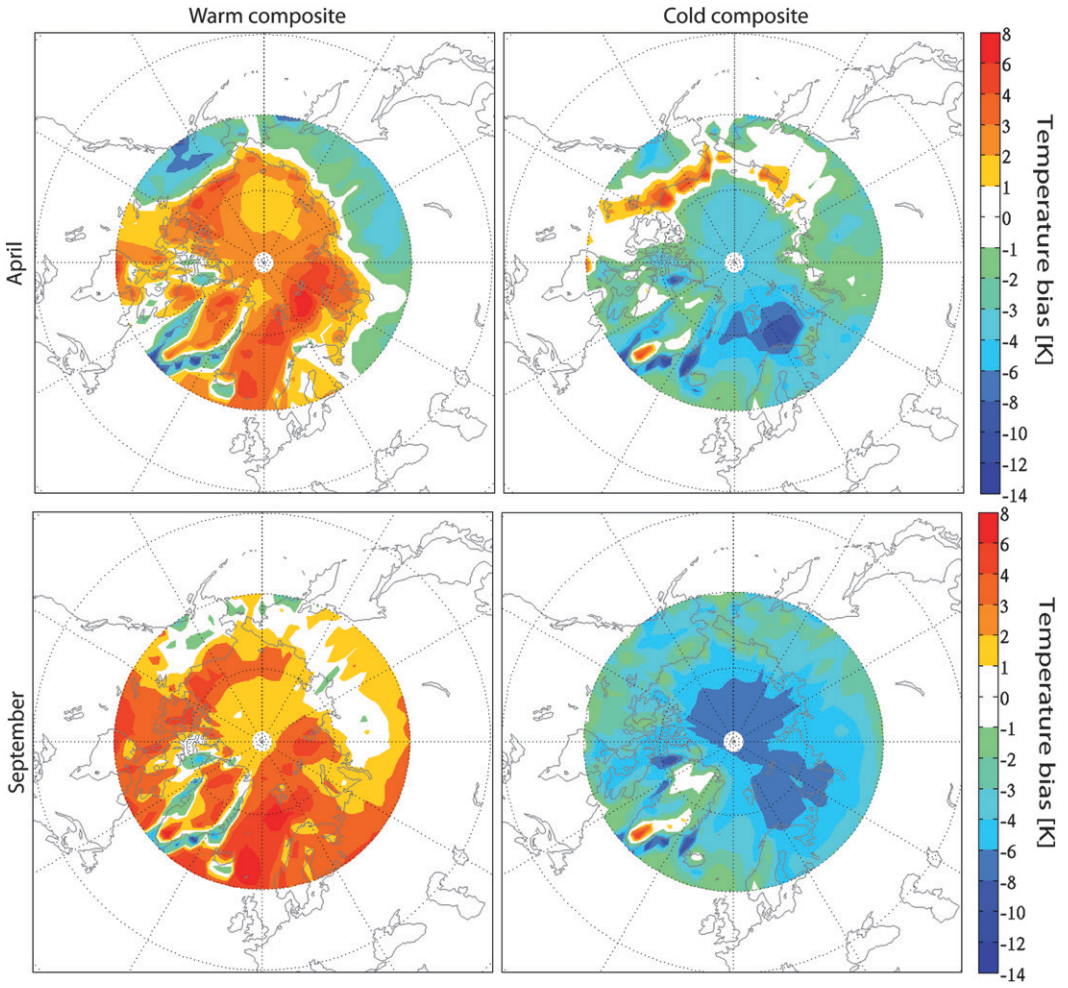

FIG. 2. Bias of the surface temperature (K) (1970–99) for the (left) warm and (right) cold composite. Shown are the biases in (top) April and (bottom) September.

surprisingly, has a greater sea ice extent than the warm composite. Similar to Fig. 2, the main differences between the two composites are over the Barents Sea. This suggests that the models simulating a smaller sea ice extent for today's climate conditions show a larger decrease of sea ice and therefore less remains in a future climate. The findings in Boé et al. (2009c) support this hypothesis. The five coldest models belong to the group of models showing the largest remaining area of September sea ice at the end of this century (Boé et al. 2009c). On the other hand, three models of the warm composite belong to the four models with the smallest area of September sea ice at the end of this century. One model of our warm composite is not used in the study by Boé et al. (2009c), and one model is in the lower half with less September sea ice left of the sample used by Boé et al. A reason for this difference could be that this model has a larger sea ice extent in the preindustrial conditions. When correlating the mean temperature bias for September in the Arctic region with the mean sea ice extent in September both for 1980–2008, it becomes evident that models with a larger bias toward warm temperature have smaller sea ice extent and vice versa, with a correlation of −0.84 as shown in Fig. 4. The reason why the models in the warm composite feature a relatively large warm bias but still simulate the sea ice extent very accurately may be due to the cold bias in the ERA-40 product over the Arctic Ocean.

The sea ice thickness in April and September clearly shows that the cold composite has thicker sea ice than the warm composite, as depicted in Fig. 5. The warm composite probably captures the sea ice thickness more realistically than the cold composite (M. Holland 2009, personal communication). Interestingly, according to the study by Holland et al. (2010), the largest scatter of sea ice thickness across the CMIP3 models is found in

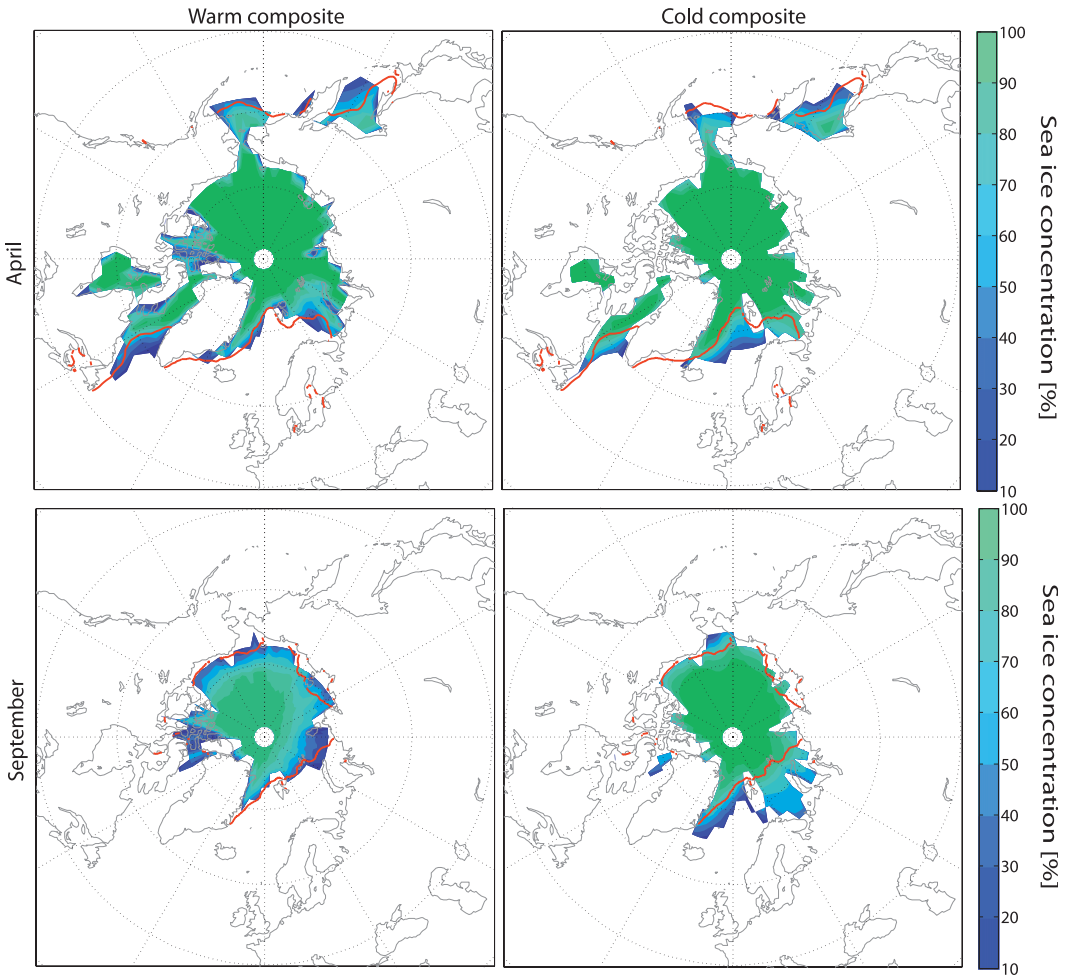

FIG. 3. Sea ice concentration (%) in (top) April and (bottom) September for 1980–2008: the (left) warm and (right) cold composite. Only sea ice concentrations greater than 15% are shown; the red line shows the 15% line of the observations (HadISST). Also, for the observations only sea ice concentrations greater than 15% are used.

the Barents Sea. The ice thickness is an important factor for the melt in spring and summer since thinner ice is more vulnerable to melting during warm periods (Holland and Bitz 2003). Generally speaking, both characteristics of Arctic sea ice—extent and thickness—are important for the processes governing the Arctic warming. In spring and summer the ice cover decreases owing to sea ice albedo feedback and the ocean absorbs shortwave radiation, which is stored as thermal energy. In fall and winter, thinning and decreasing sea ice reduces the isolation of the ocean. Therefore, more energy is transferred from the ocean to the atmosphere and hence leads to an increase in surface temperature (Robock 1985; Hall 2004). Holland et al. (2010) support this thesis by stating that models with thicker sea ice in the annual mean simulate less net longwave heat loss at the surface during winter months.

c. The role of the northward ocean heat transport

The ocean is an important factor in the climate system. In the Arctic, and especially over the Barents Sea where the surface temperature is influenced by the North Atlantic Drift Stream, which brings warm ocean water to the Arctic region, the northward ocean heat transport influences the Arctic TAS. Koenigk et al. (2009) state that differences in sea ice concentration strongly affect the ocean heat release to the atmosphere. Consequently, local and potentially large-scale climate conditions are influenced by different sea ice conditions in the Barents Sea. Jungclaus et al. (2006) conducted a modeling study showing that an enhanced northward ocean heat transport can cause a reduction in sea ice. This relation is observed across the CMIP3 models. The models simulating a stronger mean northward ocean

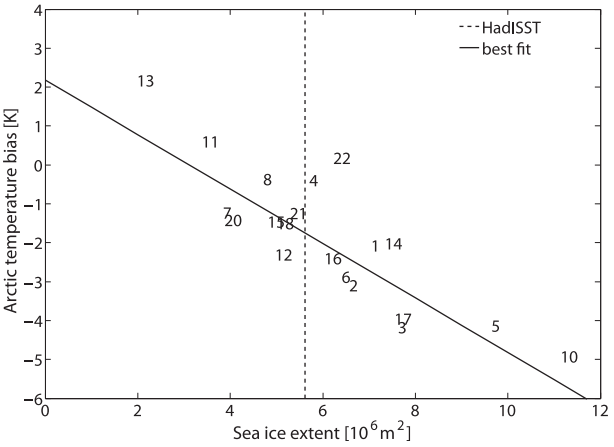

FIG. 4. Correlation ($R = -0.84$) across the CMIP3 models between the mean September surface temperature (TAS) bias (using ERA-40 as a reference) in the Arctic for 1980–2008 and the mean September sea ice extent for the same period.

heat transport, defined as the poleward flux at 60°N, show a smaller sea ice extent in September and vice versa, shown in Fig. 6. The correlation between the two quantities across the CMIP3 models is −0.72. When only the sea ice extent in the Barents Sea is used, the correlation is −0.76. Since sea ice extent is also correlated with the TAS bias (Fig. 4), the ocean heat transport is also related to the TAS bias. Hence, those models that are already too warm for today's climate will probably warm more than average in a future climate. Figure 7 shows this dependency by correlating the future warming of each model with its current northward ocean heat transport. Including all the models results in a correlation of 0.48. But excluding the outlier (model 8, the same model excluded from Fig. 1) increases the correlation to 0.68. Furthermore, the correlation between the ocean heat transport of each model with its temperature bias is 0.44. Since the TAS bias is strongly related to the sea ice extent, the northward ocean heat transport influences sea ice extent in each model. It might be surprising that the northward ocean heat transport is responsible for the large spread of the models in their future warming projections since the northward ocean heat transport contributes only a small amount to the total energy budget of the Arctic (Serreze et al. 2007). But, it has a strong influence on the sea ice extent by influencing the sea ice cover in the Barents Sea where the main differences in sea ice cover are found (Fig. 2), which in turn affects the energy budget at the surface. Our results are supported by Holland and Bitz (2003), who find a significant correlation between polar amplification and control climate ocean heat transport. The correlation of the sea ice extent of each model with its northward ocean heat transport in their study is −0.67. It is likely that increased ocean heat transport results in a thinner sea ice cover (Holland and Bitz 2003). The correlation between the northward ocean heat transport and the sea ice thickness in the Barents Sea in this study is −0.61. By influencing the sea ice extent and thickness, the northward ocean heat transport has a crucial influence on how much energy can be absorbed and stored in the ocean and, more importantly, how much of this energy is radiated back during winter. Boé et al. (2009a) find the capacity of the models to emit the stored energy in the oceans as one of the main reasons for the intermodel spread in the projections.

Meehl et al. (2000) compare two coupled climate models with different future warming and concentrate on regional processes—one of which is the sea ice mechanism. They state that ocean dynamics and heat transport significantly contribute to the model's response to sea ice developments. Additionally, they studied the changes in the ocean heat transport in a future climate and conclude that the changes in the ocean heat transport more than offset the influence on the decrease of sea ice area caused by changes in absorbed solar energy. Hence, a stronger ocean heat transport leads to a greater decrease in sea ice and therefore to a greater warming than changes in the solar radiation budget. According to Meehl et al. (2000), changes in cloud characteristics are probably not the main reason for the large spread of the models in case of Arctic warming.

Comparing the amount of heat transported by the ocean in the models and the estimates by Trenberth and Caron (2001) (Fig. 7) reveal that all but one model overestimate the northward ocean heat transport. The same findings are reported in Fig. 8.6 of Solomon et al. (2007), which shows the annual mean and zonally averaged ocean heat transport. However, observations of this parameter are difficult to obtain and large uncertainties exist. Bacon (1997) estimates the Atlantic Ocean heat transport to be 0.35 PW (cf. Fig. 7), much larger than that by Trenberth and Caron (2001), which is an estimate of the global transport. It must be noted though that almost all of the northward ocean heat at 60°N is transported to the pole by the Atlantic. Ganachaud and Wunsch (2000) estimate the transport across 50°N to be 0.6 PW. Note that the decrease of the transport between 60° and 50°N is only around a tenth of a petawatt (Trenberth and Caron 2001). Monitoring ocean heat transport remains a challenging task, but more accurate estimates might help to constrain AOGCMs in the future.

4. Conclusions

The large Arctic warming due to anthropogenic greenhouse gases and positive feedback mechanisms, which

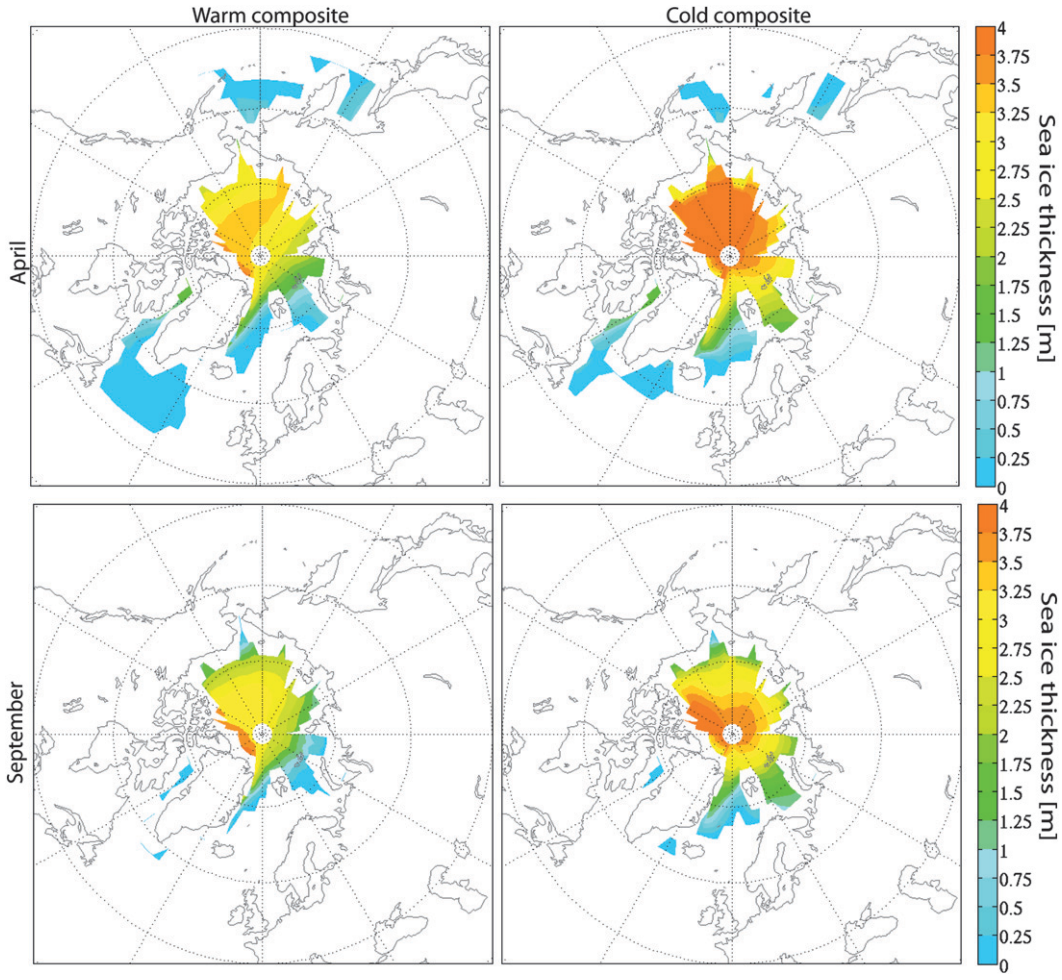

FIG. 5. Sea ice thickness (m) in (top) April and (bottom) September for 1980–2008: the (left) warm and (right) cold composite. Note that also sea ice with a concentration smaller than 15% is shown here.

cause a decrease in sea ice, have been discussed previously (Serreze and Francis 2006; Winton 2006; Wang and Overland 2009; Holland et al. 2006; Stroeve et al. 2007; Zhang and Walsh 2006); however, the key factors for the spread of the CMIP3's future projections, especially of sea ice and temperature, are still only partly known. In this study we show that large differences between the models in their simulated spatial patterns of current temperature (TAS) exist. Constructing two composites using five models showing the highest and five models showing the lowest future temperature rise in the Arctic reveals new insights into model processes. Compared to observations, the main differences can be geographically localized over the Barents Sea. This region, influenced by ocean currents and their associated northward heat transport, shows the largest differences in sea ice cover, as well as for TAS. The area covered by sea ice, however, is a major driver of the feedback mechanism in the Arctic. Furthermore, it has previously been shown that the capability of the models to radiate energy from the oceans back to the atmosphere contributes largely to the model spread of their future projections (Boé et al. 2009a). If the ocean is less covered with sea ice, it can absorb more solar radiation and energy is radiated back more effectively since sea ice functions as an insulator. Thus, the ocean heat transport plays a key role in the Arctic climate system even if its energy flux to the Arctic is relatively small. The significant role that this physical process plays in the whole climate system suggests that improving the simulation of ocean heat transport across the CMIP3 models would lead to more accurate future projections and fewer uncertainties across the models. Although interannual variability of sea ice volume in the Barents Sea depends on local winds, the oceanic heat transport is important on longer time scales (Koenigk et al. 2009). Improving model simulations of ocean heat

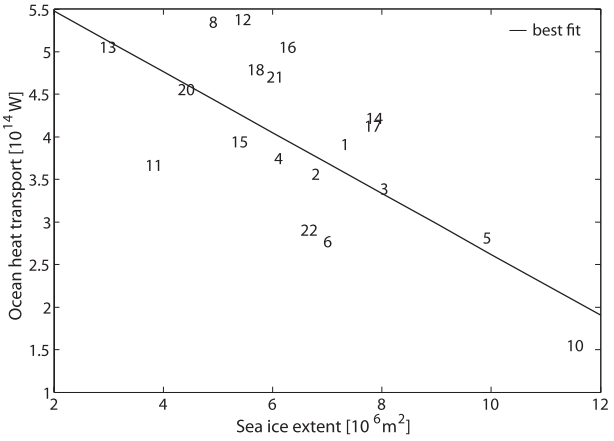

FIG. 6. Correlation ($R = -0.72$) across the CMIP3 models between the northward ocean heat transport and the sea ice extent averaged over the period 1970–99.

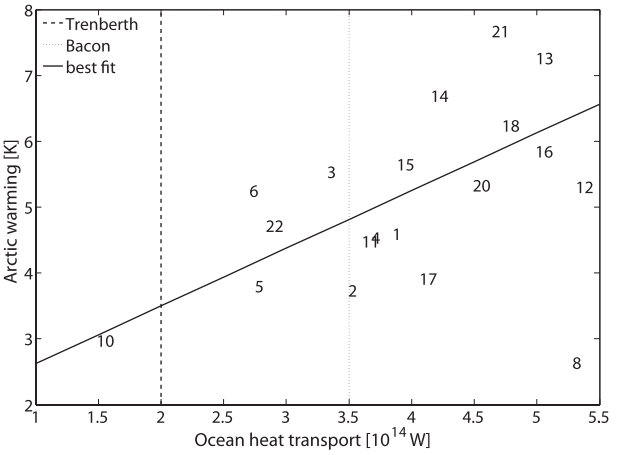

FIG. 7. Correlation ($R = 0.68$, excluding model 8) across the CMIP3 models between future Arctic warming and the mean northward ocean heat transport (1970–99). The dashed line is an estimate of the observed northward ocean heat transport by Trenberth and Caron (2001), and the dotted line is an estimate of Bacon (1997) at 60°N. The best fit excludes model 8.

transport implies studying the North Atlantic meridional overturning circulation (MOC), which affects sea ice in the Barents Sea through enhanced ocean heat transport in periods with above normal MOC (Jungclaus et al. 2006). Sea ice extent and temperatures in the Barents Sea are also related to the North Atlantic Oscillation (NAO) since positive NAO phases cause enhanced atmospheric and oceanic heat transport. Because the ocean heat transport is a result of many complex physical processes and given that measuring ocean heat transport is difficult, expensive, and requires long-term monitoring to reduce the effect of decadal variability in the ocean, it may be very challenging to improve its simulation in a climate model owing to several limitations such as model resolution, process understanding, and data limitations.

Model evaluation is not a trivial task and different approaches exist. Gleckler et al. (2008) and Reichler and Kim (2008) define an overall metric of skill by evaluating a number of variables globally. However, a ranking based only upon a single overall metric including many different variables may not be useful, as a single best model for all climate variables and regions is unlikely to exist. It is also unclear how rankings based on the present-day mean climate relate to future projections (Knutti et al. 2010; Tebaldi and Knutti 2007). This is reflected in the current IPCC Report in which all models are given equal weight and no performance metric is applied. However, a model ranking can be useful in case of an evaluation based on specific physical processes if they are shown to be relevant for a specific prediction. Some models do not meet basic performance criteria for a specific physical process (Eyring et al. 2007; van Oldenborgh et al. 2005) and, therefore, it is reasonable to exclude these models from the analysis (Knutti 2010). In this study a successful approach of model evaluation is presented based on a few key processes that can be demonstrated to control the climate of a region.

In summary we show that the northward ocean heat transport contributes largely to the uncertainty in future Arctic climate projections based on correlations across the CMIP3 models. There is always a possibility that correlations occur by chance or that they reflect that all models make similar simple assumptions. We have demonstrated that the correlations across multiple variables provide a consistent picture and can be understood in terms of physical processes. Furthermore, the climate of the Arctic is determined by multiple components and processes that are represented quite differently in the various models. We are therefore confident that the correlations are indicating real differences in the physics of the models.

Comparing the CMIP3 Arctic temperature simulations with observations suggests that the expected Arctic warming is rather at the upper end of the simulated range because mean simulated temperatures for 1981–2000 are generally 1–2 K too low compared to corresponding observations (Chapman and Walsh 2007). The Barents Sea is an exception, with a cold bias of 6–8 K (Chapman and Walsh). Increasing model resolution on average indeed leads to more accurate results in case of Arctic climate simulations. The median of the cold composite of the amount of grid cells covering the area 60°–90°N is 768 compared to 4608 of the warm composite. We showed that the warm composite models simulate the current Arctic climate more accurately than the cold composite. Note that the resolution of a model may only be part of the story, as resolution is

often also correlated with the overall complexity of a model, which will depend on the number of people working on it, experience in constructing a model, the amount of computational power, and the amount of money spent on the model development are also important factors: all are expected to be correlated with resolution. Excluding the low-resolution models in this specific case reduces the spread in future projections. This implies that true future polar warming is likely to be at the upper end of the simulated range by the CMIP3 models. The lower end of the polar warming projections is then moved up from ~2.5 to ~4 K. This means that a temperature increase of ~4–8 K is expected by the end of this century in a SRES A1B scenario.

Acknowledgments. We thank Jan Sedlacek, Susan Solomon, and Christof Appenzeller for their fruitful discussions. We also acknowledge the modeling groups—the Program for Climate Model Diagnosis and Intercomparison (PCMDI) and the WCRPs Working Group on Coupled Modeling (WGCM)—for their roles in making available the WCRP CMIP3 multimodel dataset. Support of this dataset is provided by the Office of Science, U.S. Department of Energy.

REFERENCES

Arzel, O., T. Fichefet, and H. Goosse, 2006: Sea ice evolution over the 20th and 21st centuries as simulated by current AOGCMs. *Ocean Modell.,* **12,** 401–415, doi:10.1016/j.ocemod.2005.08.002.

Bacon, S., 1997: Circulation and fluxes in the North Atlantic between Greenland and Ireland. *J. Phys. Oceanogr.,* **27,** 1420–1435.

Boé, J., A. Hall, and X. Qu, 2009a: Current GCMs' unrealistic negative feedback in the Arctic. *J. Climate,* **22,** 4682–4695.

——, ——, and ——, 2009b: Deep ocean heat uptake as a major source of spread in transient climate change simulations. *Geophys. Res. Lett.,* **36,** L22701, doi:10.1029/2009GL040845.

——, ——, and ——, 2009c: September sea-ice cover in the Arctic Ocean projected to vanish by 2100. *Nat. Geosci.,* **2,** 341–343, doi:10.1038/NGEO467.

Bromwich, D. H., R. L. Fogt, K. I. Hodges, and J. E. Walsh, 2007: A tropospheric assessment of the ERA-40, NCEP, and JRA-25 global reanalyses in the polar regions. *J. Geophys. Res.,* **112,** D10111, doi:10.1029/2006JD007859.

Chapman, W. L., and J. E. Walsh, 2007: Simulations of Arctic temperature and pressure by global coupled models. *J. Climate,* **20,** 609–632.

Deser, C., R. Tomas, M. Alexander, and D. Lawrence, 2010: The seasonal atmospheric response to projected Arctic sea ice loss in the late twenty-first century. *J. Climate,* **23,** 333–351.

Eyring, V., and Coauthors, 2007: Multimodel projections of stratospheric ozone in the 21st century. *J. Geophys. Res.,* **112,** D16303, doi:10.1029/2006JD008332.

Flato, G. M., and G. J. Boer, 2001: Warming asymmetry in climate change simulations. *Geophys. Res. Lett.,* **28,** 195–198.

Ganachaud, A., and C. Wunsch, 2000: Improved estimates of global ocean circulation, heat transport and mixing from hydrographic data. *Nature,* **408,** 453–457.

Gleckler, P. J., K. E. Taylor, and C. Doutriaux, 2008: Performance metrics for climate models. *J. Geophys. Res.,* **113,** D06104, doi:10.1029/2007JD008972.

Hall, A., 2004: The role of surface albedo feedback in climate. *J. Climate,* **17,** 1550–1568.

Holland, M. M., and C. M. Bitz, 2003: Polar amplification of climate change in coupled models. *Climate Dyn.,* **21,** 221–232, doi:10.1007/s00382-003-0332-6.

——, ——, and B. Tremblay, 2006: Future abrupt reductions in the summer Arctic sea ice. *Geophys. Res. Lett.,* **33,** L23503, doi:10.1029/2006GL028024.

——, M. C. Serreze, and J. Stroeve, 2010: The sea ice mass budget of the Arctic and its future change as simulated by coupled climate models. *Climate Dyn.,* **34,** 185–200, doi:10.1007/s00382-008-0493-4.

Jungclaus, J. H., and Coauthors, 2006: Ocean circulation and tropical variability in the coupled model ECHAM5/MPI-OM. *J. Climate,* **19,** 3952–3972.

Knutti, R., 2010: The end of model democracy? *Climatic Change,* **102,** 395–404, doi:10.1007/s10584-010-9800-2.

——, G. A. Meehl, M. R. Allen, and D. A. Stainforth, 2006: Constraining climate sensitivity from the seasonal cycle in surface temperature. *J. Climate,* **19,** 4224–4233.

——, R. Furrer, C. Tebaldi, J. Cermak, and G. A. Meehl, 2010: Challenges in combining projections from multiple climate models. *J. Climate,* **23,** 2739–2758.

Koenigk, T., U. Mikolajewicz, J. H. Jungclaus, and A. Kroll, 2009: Sea ice in the Barents Sea: Seasonal to interannual variability and climate feedbacks in a global coupled model. *Climate Dyn.,* **32,** 1119–1138, doi:10.1007/s00382-008-0450-2.

Manabe, S., and R. J. Stouffer, 1980: Sensitivity of a global climate model to an increase of CO_2 concentration in the atmosphere. *J. Geophys. Res.,* **85** (C10), 5529–5554.

Meehl, G. A., W. D. Collins, B. A. Boville, J. T. Kiehl, T. M. L. Wigley, and J. M. Arblaster, 2000: Response of the NCAR climate system model to increased CO_2 and the role of physical processes. *J. Climate,* **13,** 1879–1898.

——, C. Covey, T. Delworth, M. Latif, B. McAvaney, J. F. B. Mitchell, R. J. Stouffer, and K. E. Taylor, 2007: The WCRP CMIP3 multimodel dataset: A new era in climate change research. *Bull. Amer. Meteor. Soc.,* **88,** 1383–1394.

Murphy, J. M., D. M. H. Sexton, D. N. Barnett, G. S. Jones, M. J. Webb, M. Collins, and D. A. Stainforth, 2004: Quantification of modelling uncertainties in a large ensemble of climate change simulations. *Nature,* **429,** 768–772.

Rayner, N. A., D. E. Parker, E. B. Horton, C. K. Folland, L. V. Alexander, D. P. Rowell, E. C. Kent, and A. Kaplan, 2003: Global analyses of sea surface temperature, sea ice, and night marine air temperature since the late nineteenth century. *J. Geophys. Res.,* **108,** 4407, doi:10.1029/2002JD002670.

Reichler, T., and J. Kim, 2008: How well do coupled models simulate today's climate? *Bull. Amer. Meteor. Soc.,* **89,** 303–311.

Robock, A., 1985: An updated climate feedback diagram. *Bull. Amer. Meteor. Soc.,* **66,** 786–787.

Serreze, M. C., and J. A. Francis, 2006: The Arctic amplification debate. *Climatic Change,* **76,** 241–264, doi:10.1007/s10584-005-9017-y.

——, A. P. Barrett, A. G. Slater, M. Steele, J. Zhang, and K. E. Trenberth, 2007: The large-scale energy budget of

the Arctic. *J. Geophys. Res.,* **112,** D11122, doi:10.1029/2006JD008230.

Solomon, S., D. Qin, M. Manning, M. Marquis, K. Averyt, M. M. B. Tignor, H. L. Miller Jr., and Z. Chen, Eds., 2007: *Climate Change 2007: The Physical Science Basis*. Cambridge University Press, 996 pp.

Stroeve, J., M. M. Holland, W. Meier, T. Scambos, and M. Serreze, 2007: Arctic sea ice decline: Faster than forecast. *Geophys. Res. Lett.,* **34,** L09501, doi:10.1029/2007GL029703.

Tebaldi, C., and R. Knutti, 2007: The use of the multi-model ensemble in probabilistic climate projections. *Philos. Trans. Roy. Soc. London,* **A365,** 2053–2075, doi:10.1098/rsta.2007.2076.

Trenberth, K. E., and J. M. Caron, 2001: Estimates of meridional atmosphere and ocean heat transports. *J. Climate,* **14,** 3433–3443.

Uppala, S. M., and Coauthors, 2005: The ERA-40 Re-Analysis. *Quart. J. Roy. Meteor. Soc.,* **131,** 2961–3012.

van Oldenborgh, G. J., S. Y. Philips, and M. Collins, 2005: El Niño in a changing climate: A multi-model study. *Ocean Sci.,* **1,** 81–95.

Walsh, J. E., W. L. Chapman, V. Romanovsky, J. H. Christensen, and M. Stendel, 2008: Global climate model performance over Alaska and Greenland. *J. Climate,* **21,** 6156–6174.

Wang, M., and J. E. Overland, 2009: A sea ice free summer Arctic within 30 years? *Geophys. Res. Lett.,* **36,** L07502, doi:10.1029/2009GL037820.

Winton, M., 2006: Amplified Arctic climate change: What does surface albedo feedback have to do with it? *Geophys. Res. Lett.,* **33,** L03701, doi:10.1029/2005GL025244.

Zhang, X. D., 2010: Sensitivity of Arctic summer sea ice coverage to global warming forcing: Towards reducing uncertainty in Arctic climate change projections. *Tellus,* **62A,** 220–227.

——, and J. E. Walsh, 2006: Toward a seasonally ice-covered Arctic Ocean: Scenarios from the IPCC AR4 model simulations. *J. Climate,* **19,** 1730–1747.